Anthropogenic Impacts on Mud and Organic Carbon Cycling

+

Thomas S. Bianchi,[1] Lawrence M. Mayer,[2] Joao H. F. Amaral,[1] Sandra Arndt,[3] Valier Galy,[4] David B. Kemp,[5] Steven A. Kuehl,[6] Nicholas J. Murray,[7] and Pierre Regnier[3]

[1]Department of Geological Sciences, University of Florida, Gainesville, FL 32611 USA

[2]School of Marine Sciences, University of Maine, Walpole, ME, USA

[3]BGeoSys, Department of Geosciences, Environment and Society, Université Libre de Bruxelles, Brussels, Belgium

iC3, Center for Ice, Climate, Carbon and Cryosphere, UiT the Arctic University of Norway, Tromsø, Norway

[4]Department of Marine Chemistry and Geochemistry, Woods Hole Oceanographic Institution, Woods Hole, MA 02543, USA

[5]State Key Laboratory of Biogeology and Environmental Geology and Hubei Key Laboratory of Critical Zone Evolution, School of Earth Sciences, China University of Geosciences, Wuhan, China

[6]Virginia Institute of Marine Science, College of William and Mary, Gloucester Point, VA 23062, USA

[7]College of Science and Engineering, James Cook University, Townsville, Queensland, Australia.

Abstract:

Fine-grained muds produced largely from rock weathering at the Earth's surface, have great influence on global carbon cycling. It helps sediment bind and protect organic carbon from remineralization, and its organic loading controls the amounts, timescales, and pathways of sediment and soil organic carbon sequestration. Human activities have resulted in marked changes (both increases and decreases) in mud (mud-OC) loadings in different environments via altering organic matter (OM) reactivity. Such impacts on mud and mud-OC can be directly caused by activities such as damming and levee-building, or directly result from human-induced climate change. Here we present a synthesis of impacts of human activities on production, transfer, and storage of mud-OC. In general, we predict that anthropogenic climate warming will increase net fluxes of mud-OC in most of the systems discussed here, with uncertainties for tidal flats and flood plains, and likely net losses for coastal wetlands.

I. Introduction: Mud is the Medium

The importance of fine-grained mud in shaping Earth's climate history has stimulated broad interest in the Geosciences [1,2], with focus in the associations between mud and organic carbon (mud-OC - Box 1) beginning in the mid-19th century. Mud is a key medium that integrates the carbon cycle as initiated by rock weathering and soil erosion, followed by transport, transformation and sequestration/burial of mud-OC across diverse landscapes[3–5]. Mud has been linked with microbial evolution[6], relating it to past and future changes in weathering, biogeochemical cycles, and climate [6]. Mudrocks represent about 60% of all sedimentary rocks in

Earth's crust, and are the primary archive from which geologists reconstruct Earth's biotic and climatic history[7]. Mud's influence on Earth's carbon cycling and climate has accentuated since the Paleozoic (Supplementary Text).

Anthropogenic disturbances to mud and mud-OC cycling have likely occurred from the mid-to-late Holocene [8], with the most rapid and profound effects occurring during the Great Acceleration, or Anthropocene (e.g.,[9,10]). Human activities are now altering the production, source-to-sink transport, and fate of mud-OC via changes in land-use (e.g., deforestation, agriculture, mining, road-building), water management (e.g., damming, levees, groundwater withdrawal), perturbations of the coastal and deep ocean (dredging, trawling, offshore wind farms, aquaculture, mining), atmospheric CO_2 and climate (e.g., droughts, floods, sea-level rise, glacier retreat, permafrost thaw, terrestrial biosphere productivity). Because the fate of mud-OC can have significant impacts on greenhouse gas (GHG) fluxes and C sequestration/burial in the biosphere, important questions remain on how these anthropogenic changes will affect the C cycle and climate in the 21st century [11]. Humans have altered the transit and hence distribution of mud between its weathering sources and its depositional sinks, dramatically changing its residence time along source-to-sink gradients [12–19]. Moreover, changing environmental conditions strongly influence the inputs, processing, remineralization, and sequestration of mud-OC[20].

Here we review the state of knowledge about mobilization and storage of mud and its associated OC through dominant source-to-sink pathways (Fig. 1). We focus on Holocene-Anthropocene effects by human activities, which are altering production, transport and environmental conditions for mud-OC and therefore its exchange with pools such as the atmosphere. We emphasize mud-OC in permafrost, whose thawing mud fluxes from land to sea in the Arctic (e.g.,[4]). Our main objectives are to: 1) assess how the dominant drivers of mud-OC production have changed over the Holocene-Anthropocene; 2) provide overview of the large spatial and temporal changes of where mud-OC is remineralized and buried along the land-to-sea pathway, with potential consequences for carbon cycling and climate; and 3) explore how understanding of the fate of mud-OC can help predict consequences such as recently accelerated release of ancient petrogenic and permafrost-derived OC to the biosphere.

II. The modern mud-OC cycle on land

Production of mud-OC in terrestrial ecosystems

Mud production requires weathering reactions, which change both particulate and dissolved materials (e.g., feldspar to clay minerals and consequent increase in dissolved silica and various ions). Mass budgets of mud are dominated by transfers among pre-existing mud deposits [12] (e.g., soils and sediments) among different parts of the landscape - not new production of mud-sized minerals. Monitoring of dissolved ions to assess global weathering does not indicate Anthropocene increase in mud-producing reactions [12].

Despite little change in total available mud, erosion of mud-OC from ice-free landscapes in temperate regions has been significantly affected by land-use change over the Holocene-Anthropocene. Human agriculture has significantly increased global soil denudation since the late Holocene; an estimated ~36 Pg yr^{-1} of soil was eroded in 2012 [13]. Currently, an estimated 37% of all ice-free land is directly used for agriculture and human settlements [14,15]. Impacts are most pronounced in the northern hemisphere, which hosts more land, human population, and gross domestic product [13,15]. Soil loss and mud-OC mobilization due to anthropogenic land-use changes began >4000 years ago [8,17]. In North America, the impact of European colonization on the landscape (via agriculture and river modifications) is readily observed, with rates of surficial sediment movement (and hence mud-OC mobilization) over the past century about 10 times higher than pre-colonial rates [16]. Rates of deforestation and agricultural land expansion are now slowing or even reversing in the northern hemisphere, and accelerating in the southern hemisphere [18]. In Europe, climate change rather than land-use change is predicted to be the main driver of modest increases in soil erosivity in coming decades [19]. Global land-surface models integrating vegetation dynamics suggest that enhanced plant growth driven by increased atmospheric CO_2 could partly mitigate the erosive effects of climate change via soil stabilization [21]. In contrast, significant late 20th and 21st-century increases in land-use changes in South America, Africa, and Southeast Asia have made these tropical areas the main loci of soil erosion, with rates predicted to substantially increase in the near future [13]. Human-induced, extreme precipitation/flooding events are also predicted to increase in many regions across the world (e.g., [22]), affecting erosion rates and the fate of mud-OC [12].

Fate of mud-OC along the global inland water network

Humans clearly affect mobilization, processing and storage of mud-OC in the transit from soils to the ocean, especially via residence time of mud in different parts of the system [3,23–25]. Dam proliferation in North America, Europe/Eurasia, and Asia since the 1950s is generally believed to be starving the coast of sediment (Supplementary Fig. 1). In contrast, sediment transport in 39% of rivers in South America, Africa and Oceania has increased since the 1980s due to land-use changes, especially deforestation[26]. Current estimates indicate a 49% global reduction in fluvial sediment reaching the oceans despite a >200% increase in upstream fluvial sediment loads, between 1950 and 2010 [12,26]. Dams can trap (Figs. 1, 2c and Table 1) mud-OC (60, range 20-70 $TgCyr^{-1}$) [27], the magnitude of which depends upon specific environmental and hydrological conditions (e.g., [27,28]). For instance, dams strongly stimulate phytoplanktonic production within the global inland water network, but also the mineralization of both fresh organic matter (OM) and terrestrial-derived material; thus these systems exhibit a highly variable, net heterotrophic status at global scale [28]. Dam construction up to 1970 eliminated 8% of the total riverine OC flux through burial and mineralization, and this removal rate is expected to have more than doubled (to 19% in 2030) with dams either completed or planned after 1970 [28]. Furthermore, the interruption of sediment flux by dams increases net downstream erosion (Fig. 2c), which can partially offset mud-OC trapping until the river profile re-equilibrates (e.g., [29]). Lakes without dams are also important hotspots of mud-OC burial (90, range, 40–180 $TgCyr^{-1}$) (Fig. 1 and Table1) although significantly less efficient on an areal basis than reservoirs with higher sedimentation rates and better conditions for OC preservation (e.g. anoxia, Box 2) [27]. Moreover, several regional studies suggest a significant increase in lake mud-OC burial since pre-industrial times [5]. Northern-Hemisphere lakes have increased OC burial by about 50% over the last century (Fig 2c), possibly due to the combined effects of climate change and enhanced terrestrial productivity [30]. Present-day OC accumulation rates in European lakes are double those of the Holocene, mostly attributed to land-use change [31].

River floodplains are key areas of storage, processing, and release of mud-OC, affecting OC:specific surface area (SSA) values and OC reactivity. As with reservoirs, they lead to mixtures of new and "aged" materials [3,4]. In contrast to lakes and reservoirs for which global assessments of long-term burial are available (e.g.,[27]), the amount of mud-OC sequestered in floodplain systems is highly uncertain but possibly of similar magnitude (190, range 60-320 $TgCyr^{-1}$) [5,32] as in lentic bodies (150, range 60-250 $TgC\ yr^{-1}$) (Fig. 1 and Table 1). Natural floodplains store and release mud via overbank sedimentation and river channel migration/river bank erosion, respectively, as well as other climate-driven fluctuations in the hydrological cycle (e.g., La Niña and El-Niño). Deposition and residence time increase as a result of large floods and decrease during droughts. Levee construction interrupts this process, often by reducing connectivity between rivers and their floodplains (e.g.,[33]). Increased erosion from human activities may reduce mud residence times in the land-ocean transition (Fig. 2b), but creation and isolation of floodplains has the opposite effect [34]. The net effects of human activities on the floodplain mud-OC cycle remain largely unknown at the global scale (see [5]). While the composition of mud minerals varies relatively little during the long transit from source-to-sink, as evidenced by similar oceanic and adjacent terrestrial clay mineral suites [35–37], the composition of mud-OC is more variable. Much mud-OC is decomposed in floodplains in its transit [24,38]. Along the entire source-to-sink transition, but particularly in the floodplain, petrogenic OM is partially replaced by OC from land plants and river/lake phytoplankton (e.g.,[24,28]). Addition of fresh OM may prime the degradation and replacement observed in floodplains [39].

Changes in fluvial morphology affect the fate of mud-OC by altering water dynamics, residence time, redox conditions, turbidity, particle size/density, and mineral/OC sources [40] Agricultural expansion in river networks in China (1960s-1980s) enhanced erosion resulted in loss of high order rivers to sediment infilling [41]. During later urbanization (1980s-2010s), when ca. 40% of some natural landscapes reached a status of "urbanized" (e.g., extensive dredging and reconstruction of high order rivers), lower order rivers experienced sediment infilling. The importance of changing floodplain topography on mud-OC cycling remains largely unexplored (e.g.,[42]). Creation of reclaimed agricultural land such as rice paddies (Supplementary Fig. 1) can enhance OC:SSA ratios several-fold [43]. Greater predictability in the land use-driven changes in river channel evolution and spatial-temporal dynamics of erosion and sedimentation across watersheds [44] will provide consistent frameworks to assess changes in mud-OC [45].

III. Production, transfer, and storage of mud-OC in nearshore

In addition to impacts on terrestrial sediment and mud-OC fluxes, damming has contributed to coastal erosion (Fig. 2) in many of the world's larger deltas (e.g., with areas >1,000 km^2 such as the Mississippi, Mekong, etc.) [46], which are sinking several times faster than smaller deltas because they house more dams, contain a higher fraction of mud, are extensively modified by humans, and are large enough to induce isostatic subsidence [12]. In contrast, many (mostly smaller) coastal deltas have grown over recent decades, largely due to increases in fluvial-derived sediment linked to deforestation [47]. Century-long records show a doubling of sediment accumulation rates in most North American coastal depocenters apart from the Mississippi delta region, facilitated by erosion downstream (Fig. 2c) of dams [48].

Coastal deltas and estuaries (Fig. 2a,b) are key depositional and processing environments of mud-OC along the source-to-sink transition, where unidirectional river flow interfaces with tidal and wave processes (e.g.,[49]). Despite complexity among coastal regions, sea-level rise and extensive coastal development have resulted in net global decrease in mudflat area, primarily in temperate and low-latitude regions (Supplementary Fig. 1) [50]. Over two decades (1999 - 2019), an estimated 13,700 km^2 of tidal wetlands were lost globally, offset by gains of 9700 km^2, for a global net loss of −4000 km^2 [51]. Coastal wetlands (Fig. 2a), which commonly host "blue carbon" (e.g., mangroves, tidal marshes, and seagrasses) (Supplementary Fig. 1), can have very high OC:SSA values (e.g., up to 34 mg-OC m^{-2} [52,53]) and have some of the highest rates of short-term C sequestration and mud-OC burial (e.g., [54]), with a global assessment reaching 60 (range 40-80) TgC yr^{-1} [5] (Fig. 1 and Table 1).

In fast-warming Pan-Arctic latitudes, permafrost thaw and thermo-erosional features in nearshore coastal regions have remobilized soils and changed source-to-sink movement of mud-

OC (e.g.,[55,56]). While the range of grain size in permafrost can be quite variable, recent studies have shown that the majority of soil organic carbon in permafrost across the Arctic is in the mud fraction [57,58]. Warming air and sea temperatures, sea-level rise and longer open-water seasons have enhanced Pan-Arctic erosion and mobilization by 14 Tg OC yr^{-1} from permafrost soils to the aquatic continuum [55,59] (Figs. 1, 2d and Table 1). In turn, the mobilization of this old mud-OC and associated nutrients sustains a significant fraction of Arctic primary production and supply of new fresh OM [60]. Much of the permafrost OC is comprised of silty mud-OC draining from nearshore erosion of retrogressive thaw slumps and bluffs/cliffs [61]. Mud-OC export from retrogressive thaw slumps, which typically extend farther inland than cliffs, may take decades to hundreds of years, compared to days-months from cliffs, before reaching the Arctic Ocean [55]. These differences in OC release result in a slower and steady conversion to CO_2 from retrogressive thaw slumps, compared to more rapid pulses of cliff-derived mud-OC release [55]. Pan-Arctic nearshore coastal systems also provide more targeted zones for examining the impact of ocean phytoplankton on the fate of permafrost-derived mud-OC in a warming climate. For example, mud-OC in deep waters of non-glaciated fjords of southeastern Alaska is largely undegraded with modern radiocarbon ages (biospheric sources) - due to inputs of phytoplankton [62]. In contrast, nearby glaciated fjords are starved of phytoplankton and bury significant amounts of petrogenic OC and terrigenous biospheric OC (Fig. 2d). Similar to cliff and retrogressive thaw slump systems, Arctic deltas represent an important land-sea interface, where thawed, millennial-aged, permafrost-derived mud-OC is processed. For example, permafrost-derived mud-OC in the Colville River delta, Alaska, originates from bank erosion in upstream tributaries in the basin [56] (Fig. 2d). How glacial retreat in the Arctic will impact mud-OC burial, will largely depend on regional differences in sedimentation rates, the relative inputs of older terrestrial sources (e.g., petrogenic, permafrost) versus younger marine (macro-and microalgal), differential binding of these OC sources to minerals, and the response of microbial community to these changing pools.

Accommodation space in nearshore coastal ecosystems

Accommodation space is space available for vertical mineral and organic material accumulation in nearshore ecosystems (e.g., coastal wetlands, deltas, estuaries, inner shelves). It is largely controlled by relationships among sea-level, sediment accumulation rate, and vertical ground motion (e.g., isostatic adjustment, tectonics, subsidence/sediment compaction, and fluids withdrawal) (e.g.,[63]) (Figs. 1, 2 a,b). However, dramatic anthropogenic alterations in the delivery of fluvial sediments to the coast [12] and structures from human development [64] also change available accommodation space – which affects potential storage and turnover of mud-OC (Figs. 2 a,b).

Modeling and empirical data suggest that accommodation space is a key variable determining coastal wetland habitat (Fig. 2a) expansion during sea-level rise (SLR) over the past few millennia [65,66]. Recent models show that, over the past ca. 4,200 years, tidal marshes in regions with more rapid declining relative SLR (RSLR) (e.g., Europe and North America) had greater OC concentration than in regions with slower declining RSLR (e.g., Africa, Australia, China and South America) [67]. In the case of the Northern Hemisphere, where RSLR has been decelerating, vertical and lateral accommodation space was created over time [68], due to greater inundation frequency which allowed for higher mud-OC accumulation [66]. Controls on accommodation space are further complicated in large deltaic regions experiencing anthropogenic disturbances (Figs. 1 and 2b). For example, these regions experience high rates of erosion and subsidence, largely due to upstream damming and deltaic activities such as fossil fuel and groundwater extraction, respectively (e.g.,[69]). The synergistic effects of damming and subsidence increase RSLR in these deltaic regions, and further complicate modeling efforts of changing lateral and vertical accommodation space and associated mud-OC storage [70]. Damming also enhances accommodation space for storage of mud-OC in reservoirs (Figs. 1 and 2c).

Accommodation space in the Arctic coastal zone is also changing, as many glaciers (Figs. 1, 2d, and Table 1), especially tidewater glaciers, experience rapid retreat [71]. This retreat poses new questions of how plant colonization will impact the erosion and development of soils, and hence mud-OC, in newly exposed proglacial deposits (sometimes termed paraglacial) [72,73]. For example, the development of coastal landforms (deltas, cliffs, tidal flats, beaches) in proglacial deposits over the past 100 years in Svalbard, Norway [74] provides new accommodation space for producing and processing mud-OC in the Arctic (Fig. 2d), and over relatively short periods of time (10^{-1} to 10^{2} yr). Tidal glacier retreat creates proglacial landforms that potentially increase accommodation space, which can then increase residence time (in part, stabilized by shrubification) and microbial processing of mud-OC in source-to-sink transport. Newly exposed glacial sediment can show rapid increase in OC:SSA ratios [75]. To date, much of what is known about primary succession of plants in these temperate-to-arctic environments is from dated chronosequences from post-glacial retreat following the Little Ice Age (LIA)[76].

IV. Production, transfer, and storage of mud-OC in offshore

Muddy ocean deposits dominate longer-term processing and storage of mud-OC [23]. Organic loadings per unit of mud, as indicated by OC:SSA ratios, vary among depositional sites within an ocean margin region, depending on local ratios of supply vs. degradation rates of mud-OC [3,77]. The burial or oxidation fate of enormous quantities of terrigenous OC depends on local oceanographic conditions. For example, the 1600-km long inner shelf mud belt that moves from the mouth of the Amazon River to the Orinoco delta efficiently oxidizes terrigenous mud-OC, as energetic transport lowers OC:SSA ratios several fold via frequent resuspension and re-oxidation of the seabed [78]. In contrast, the offshore Ganges-Brahmaputra and Congo River outflows exhibit seaward escape of sediment via turbidity currents in submarine canyons and efficient terrigenous mud-OC burial on the adjacent deep sea fan [24]. One of the more dramatic examples of human impacts on the distribution of mud-OC is the state change from actively accreting to eroding, expansive shelf mud blankets. For example, humans and climatic variations interacted to control Holocene mud flux from mid-latitude Chinese loess hills to the adjacent ocean margin [79]. Recently, the underwater delta off the Yangtze has been rapidly eroding in response to river damming that captures sediment upstream [80], and which will surely impact biogeochemical processes and elemental fluxes for the East China Sea. Future planned dams in the Amazon basin will likely dampen the extensive offshore mobile mud-belts and mud-OC oxidation [81].

Along the ocean margins, the human impacts on mud-OC burial driven by changes in terrigenous OC deliveries are confounded by anthropogenic perturbations to ocean phytoplanktonic productivity. These include the effects of a changing physical climate and changes in nutrient inputs from atmospheric and riverine sources. Although it has long been advocated that human activities have stimulated ocean productivity and OC burial in the shallow portions of the ocean (e.g., [82]), only recently have these impacts been quantified using physically-resolved, ocean biogeochemistry models [83]. Results suggest that over the Anthropocene, net coastal ocean productivity increased by 14% as a result of nutrient inputs, and higher in hotspot regions such as the East China Sea, southern North Sea, Louisiana shelf, and shelves of the Bay of Bengal [83]. These results confirm reported widespread increases in biological productivity and eutrophication in coastal regions over the past century [84], likely inducing greater export, deposition and burial of mud-OC. With low confidence, the effects of a changing physical climate in the coastal ocean appear limited so far. The confounding effects of changing terrestrial and marine C cycles driven by multiple human factors (land-use change, climate, atmospheric CO_2, nutrient supply) make quantitative assessment of net changes in OC storage in muddy ocean sediments challenging [5]. Elevated OC:SSA ratios are evident in smaller eutrophied areas such as Long Island Sound [77], but not in larger, more exposed environments such as the East China Sea or Mississippi delta [85]. This contrast suggests human impacts on OC decay may be more important than those on OC supply.

V. Mud-OC reactivity across changing source-to-sink gradient

First order degradation rate constants (k for a first order rate law of the type: $dG/dt=-k \cdot G$ with k denoting the first order rate constant and G the OM concentration of natural OM vary by many orders of magnitude, with a strong inverse relationship over 12 orders of magnitude of time in which OM is exposed to oxidizing or remineralizing conditions [86,87] (Fig. 3). This global observation broadly supports the widely accepted "aged OC is refractory relative to recently produced OC" paradigm. It does not directly provide a mechanistic explanation of the long-term persistence of OC in the environment, though it can be summarized via integrative parameters such as energies of activation[88]. Superimposed on this broad trend is 1-3 orders of magnitude variation in reactivity at any given time of exposure. This variation is likely due in part to varying definitions of time and reactivity arising from different data sources or models. It is also certainly subject to a plethora of different factors such as OM composition, electron acceptor availability, benthic microbial community composition, physical and physicochemical protection, temperature, microbial inhibition by specific chemicals, priming, and macrobenthic activity (e.g. [89], references therein). Nevertheless, apparent reactivity provides an averaging dynamic parameter, accounting for interactions of compositional and environmental effects (Box

2). Interactions between mud and mud-OC seem to be particularly important on degradation time scales longer than 10^0-10^1 yr [90] that are particularly important to carbon sequestration [88].

Accelerated human activity in the Anthropocene acts on these reactivity controls. Climate shifts can thaw permafrost mud-OC and enhance microbial decay, or stratify water columns that can deplete bottom waters of oxygen and slow microbial attack under quiescent or resuspension conditions (e.g.,[91]). Shunting mud into zones subject to fresh OM inputs – such as eutrophic coastal waters, dammed reservoirs, or floodplains – can enhance reactivity of aged mud-OC via priming[39]. Such upshifts and downshifts of reactivity have potentially large impacts on mud-OC reactivity, coupled to residence time changes in different depocenters.

VI. Concluding Remarks

Mud-OC has generally accumulated under longer timescales than the Anthropocene ones in which human activities are destabilizing this pool. These recent changes have created a non-steady state situation that contrasts substantially with the mid-Holocene when climate conditions (and erosion processes) were more stable [8,92]. Furthermore, human impacts have led to the "release" of petrogenic mud-OC, via destabilization and erosion of the landscape, into the modern carbon cycle [4,93]. While much has been discussed about the thaw and release of millennial-aged OC in high latitudes and its consequences for climate, only recently have we begun to consider the impact of the mixing of ancient and modern biospheric OC pools, to help answer why global burial of OC is much higher than can be explained by only considering modern biospheric OC [4,5].

Mud holds most sequestered OC and exerts an important control on both OC transport and reactivity. The spatiotemporal history of mud in source-to-sink systems controls their respective net C budget over a wide range of timescales. On geologic timescales, the balance between the oxidation of petrogenic mud-OC and the formation/stabilization of biospheric mud-OC can tip source-to-sink systems from net carbon sinks (e.g., [69] Ganges-Brahmaputra) to net carbon sources (e.g., Taiwan;[94]). Over much shorter, human timescales, the Great Acceleration [9,10] has caused significant shifts in the environments of the mud medium, leading to rapid changes in its mud-OC content and composition. While grain-size normalization illuminates mud-OC changes in any grain-size matrix, future research might emphasize areas where large OC fluxes are especially affected by humans – e.g., muddy parts of floodplains (Fig. 1). Determination of changes in mud-OC content, source and composition relative to the conservative medium – rather than simple relocation of mud (e.g.,[95]) – will allow better accounting for dynamic C reservoirs such as blue carbon, with implications for our ability to predict the global short-term evolution of organic carbon reservoirs and attendant trends in atmospheric CO_2 levels. New analytical methods geared towards obtaining fine scale characterizations of the interactions between mud and mud-OC (e.g., MAOC, Fe-OC, Split Flow Thin Cell Technique) as well as data aggregation tools are leading to global-scale quantification of these disturbances to previous values. We predict that anthropogenic climate warming will increase net fluxes and burial of mud-OC in most in mountain glaciers, from land erosion, dam and lake reservoirs, river export, permafrost thaw, ice sheet erosion, coastal margins, with uncertainties for tidal flats and flood plains, and likely net losses for coastal wetlands. Depending upon available accommodation space with sea level rise. Along with changing fluxes ????

References:

1. Deevey, E. S. In defense of mud. *Bull. Ecol. Soc. Am.* **51**, 5–8 (1970).
2. Malakoff, D. Mud. *Science* **369**, 894–895 (2020).

3. Blair, N. E. & Aller, R. C. The fate of terrestrial organic carbon in the marine environment. *Annu. Rev. Mar. Sci.* **4**, 401–423 (2012).
4. Eglinton, T. I. *et al.* Climate control on terrestrial biospheric carbon turnover. *Proc. Natl. Acad. Sci.* **118**, e2011585118 (2021).
5. Regnier, P., Resplandy, L., Najjar, R. G. & Ciais, P. The land-to-ocean loops of the global carbon cycle. *Nature* **603**, 401–410 (2022).
6. Falkowski, P. G., Fenchel, T. & Delong, E. F. The microbial engines that drive Earth's biogeochemical cycles. *science* **320**, 1034–1039 (2008).
7. Blatt, H. Sedimentary petrology. (1982).
8. Jenny, J.-P. *et al.* Human and climate global-scale imprint on sediment transfer during the Holocene. *Proc. Natl. Acad. Sci.* **116**, 22972–22976 (2019).
9. Syvitski, J. *et al.* Extraordinary human energy consumption and resultant geological impacts beginning around 1950 CE initiated the proposed Anthropocene Epoch. *Commun. Earth Environ.* **1**, 1–13 (2020).
10. Zhang, T. *et al.* Warming-driven erosion and sediment transport in cold regions. *Nat. Rev. Earth Environ.* **3**, 832–851 (2022).
11. Rosentreter, J. A. *et al.* Coastal vegetation and estuaries are collectively a greenhouse gas sink. *Nat. Clim. Change* **13**, 579–587 (2023).
12. Syvitski, J. *et al.* Earth's sediment cycle during the Anthropocene. *Nat. Rev. Earth Environ.* **3**, 179–196 (2022).
13. Borrelli, P. *et al.* An assessment of the global impact of 21st century land use change on soil erosion. *Nat. Commun.* **8**, 1–13 (2017).

14. Ellis, E. C. *et al.* Used planet: A global history. *Proc. Natl. Acad. Sci.* **110**, 7978–7985 (2013).

15. Klein Goldewijk, K., Beusen, A., Doelman, J. & Stehfest, E. Anthropogenic land use estimates for the Holocene–HYDE 3.2. *Earth Syst. Sci. Data* **9**, 927–953 (2017).

16. Kemp, D. B., Sadler, P. M. & Vanacker, V. The human impact on North American erosion, sediment transfer, and storage in a geologic context. *Nat. Commun.* **11**, 6012 (2020).

17. Zhang, F. *et al.* Human Impacts Overwhelmed Hydroclimate Control of Soil Erosion in China 5,000 Years Ago. *Geophys. Res. Lett.* **49**, e2021GL096983 (2022).

18. Winkler, K., Fuchs, R., Rounsevell, M. & Herold, M. Global land use changes are four times greater than previously estimated. *Nat. Commun.* **12**, 1–10 (2021).

19. Panagos, P. *et al.* Projections of soil loss by water erosion in Europe by 2050. *Environ. Sci. Policy* **124**, 380–392 (2021).

20. Li, G. *et al.* Dam-triggered organic carbon sequestration makes the Changjiang (Yangtze) river basin (China) a significant carbon sink. *J. Geophys. Res. Biogeosciences* **120**, 39–53 (2015).

21. Zhang, H. *et al.* Global changes alter the amount and composition of land carbon deliveries to European rivers and seas. *Commun. Earth Environ.* **3**, 245 (2022).

22. Pörtner, H. O. *et al.* Climate change 2022: impacts, adaptation and vulnerability. (2022).

23. Bianchi, T. S. *et al.* Centers of organic carbon burial and oxidation at the land-ocean interface. *Org. Geochem.* **115**, 138–155 (2018).

24. Galy, V. *et al.* Efficient organic carbon burial in the Bengal fan sustained by the Himalayan erosional system. *Nature* **450**, 407–410 (2007).

25. Kuehl, S. A. *et al.* Asia's mega rivers: Common source, diverse fates. *Eos* **101**, 1–8 (2020).

26. Dethier, E. N., Renshaw, C. E. & Magilligan, F. J. Rapid changes to global river suspended sediment flux by humans. *Science* **376**, 1447–1452 (2022).
27. Mendonca, R. *et al.* Hydroelectric carbon sequestration. *Nat. Geosci.* **5**, 838–840 (2012).
28. Maavara, T., Lauerwald, R., Regnier, P. & Van Cappellen, P. Global perturbation of organic carbon cycling by river damming. *Nat. Commun.* **8**, 1–10 (2017).
29. Charoenlerkthawin, W. *et al.* Effects of dam construction in the Wang River on sediment regimes in the Chao Phraya River Basin. *Water* **13**, 2146 (2021).
30. Heathcote, A. J., Anderson, N. J., Prairie, Y. T., Engstrom, D. R. & Del Giorgio, P. A. Large increases in carbon burial in northern lakes during the Anthropocene. *Nat. Commun.* **6**, 1–6 (2015).
31. Kastowski, M., Hinderer, M. & Vecsei, A. Long-term carbon burial in European lakes: Analysis and estimate. *Glob. Biogeochem. Cycles* **25**, (2011).
32. Hoffmann, T. O. Carbon Sequestration on Floodplains. in *Treatise on Geomorphology (Second Edition)* (ed. Shroder, J. (Jack) F.) 458–477 (Academic Press, 2022). doi:10.1016/B978-0-12-818234-5.00069-9.
33. Grill, G. *et al.* Mapping the world's free-flowing rivers. *Nature* **569**, 215–221 (2019).
34. Lewin, J. & Ashworth, P. J. The negative relief of large river floodplains. *Earth-Sci. Rev.* **129**, 1–23 (2014).
35. Lalonde, K., Mucci, A., Ouellet, A. & Gélinas, Y. Preservation of organic matter in sediments promoted by iron. *Nature* **483**, 198–200 (2012).
36. Repasch, M. *et al.* Fluvial organic carbon cycling regulated by sediment transit time and mineral protection. *Nat. Geosci.* **14**, 842–848 (2021).

37. Repasch, M. *et al.* River Organic Carbon Fluxes Modulated by Hydrodynamic Sorting of Particulate Organic Matter. *Geophys. Res. Lett.* **49**, e2021GL096343 (2022).
38. Scheingross, J. S. *et al.* The fate of fluvially-deposited organic carbon during transient floodplain storage. *Earth Planet. Sci. Lett.* **561**, 116822 (2021).
39. Bianchi, T. S. The role of terrestrially derived organic carbon in the coastal ocean: A changing paradigm and the priming effect. in *Proceedings of the National Academy of Sciences* vol. 108 19473–19481 (2011).
40. Grant, K. E., Galy, V. V., Haghipour, N., Eglinton, T. I. & Derry, L. A. Persistence of old soil carbon under changing climate: The role of mineral-organic matter interactions. *Chem. Geol.* **587**, 120629 (2022).
41. Wu, L. *et al.* Impacts of land use change on river systems for a river network plain. *Water* **10**, 609 (2018).
42. Aufdenkampe, A. K. *et al.* Riverine coupling of biogeochemical cycles between land, oceans, and atmosphere. *Front. Ecol. Environ.* **9**, 53–60 (2011).
43. Wissing, L. *et al.* Organic carbon accumulation on soil mineral surfaces in paddy soils derived from tidal wetlands. *Geoderma* **228**, 90–103 (2014).
44. Julian, J. P., Wilgruber, N. A., de Beurs, K. M., Mayer, P. M. & Jawarneh, R. N. Long-term impacts of land cover changes on stream channel loss. *Sci. Total Environ.* **537**, 399–410 (2015).
45. Golombek, N. Y. *et al.* Fluvial organic carbon composition regulated by seasonal variability in lowland river migration and water discharge. *Geophys. Res. Lett.* **48**, e2021GL093416 (2021).

46. Tessler, Z. D., Vörösmarty, C. J., Grossberg, M., Gladkova, I. & Aizenman, H. A global empirical typology of anthropogenic drivers of environmental change in deltas. *Sustain. Sci.* **11**, 525–537 (2016).
47. Nienhuis, J. H. *et al.* Global-scale human impact on delta morphology has led to net land area gain. *Nature* **577**, 514–518 (2020).
48. Rodriguez, A., McKee, B., Miller, C., Bost, M. & Atencio, A. Coastal sedimentation across North America doubled in the 20th century despite river dams. *Nat. Commun.* **11**, 1–9 (2020).
49. van de Lageweg, W. I., Braat, L., Parsons, D. R. & Kleinhans, M. G. Controls on mud distribution and architecture along the fluvial-to-marine transition. *Geology* **46**, 971–974 (2018).
50. Murray, N. J. *et al.* The global distribution and trajectory of tidal flats. *Nature* **565**, 222–225 (2019).
51. Murray, N. J. *et al.* High-resolution mapping of losses and gains of Earth's tidal wetlands. *Science* **376**, 744–749 (2022).
52. Pinsonneault, A. J. *et al.* Dissolved organic carbon sorption dynamics in tidal marsh soils. *Limnol. Oceanogr.* **66**, 214–225 (2021).
53. Ilgen, A. G. *et al.* Shales at all scales: Exploring coupled processes in mudrocks. *Earth-Sci. Rev.* **166**, 132–152 (2017).
54. Macreadie, P. I. *et al.* The future of Blue Carbon science. *Nat. Commun.* **10**, 1–13 (2019).
55. Tanski, G. *et al.* Permafrost carbon and CO2 pathways differ at contrasting coastal erosion sites in the Canadian Arctic. *Front. Earth Sci.* 207 (2021).

56. Zhang, X. *et al.* Recent warming fuels Increased organic carbon export from Arctic permafrost. *AGU Adv.* **2**, e2021AV000396 (2021).

57. Schirrmeister, L. The genesis of Yedoma Ice Complex permafrost – grain-size endmember modeling analysis from Siberia and Alaska. *EG Quat. Sci. J.* **69**, 33–53 (2020).

58. Palmtag, J. & Kuhry, P. Grain size controls on cryoturbation and soil organic carbon density in permafrost-affected soils. *Permafr. Periglac. Process.* **29**, 112–120 (2018).

59. Vonk, J. E. Activation of old carbon by erosion of coastal and subsea permafrost in Arctic Siberia. *Nature* **489**, 137–140 (2012).

60. Terhaar, J., Lauerwald, R., Regnier, P., Gruber, N. & Bopp, L. Around one third of current Arctic Ocean primary production sustained by rivers and coastal erosion. *Nat. Commun.* **12**, 169 (2021).

61. Cunliffe, A. M. *et al.* Rapid retreat of permafrost coastline observed with aerial drone photogrammetry. *The Cryosphere* **13**, 1513–1528 (2019).

62. Cui, X., Bianchi, T. S., Jaeger, J. M. & Smith, R. W. Biospheric and petrogenic organic carbon flux along southeast Alaska. *Earth Planet. Sci. Lett.* **452**, 238–246 (2016).

63. Jervey, M. T. Quantitative Geological Modeling of Siliciclastic Rock Sequences and Their Seismic Expression. in *Sea-Level Changes: An Integrated Approach* (ed. Wilgus, C. K.) vol. 42 0 (SEPM Society for Sedimentary Geology, 1988).

64. Enwright, N. M., Griffith, K. T. & Osland, M. J. Barriers to and opportunities for landward migration of coastal wetlands with sea-level rise. *Front. Ecol. Environ.* **14**, 307–316 (2016).

65. Rogers, K. Accommodation space as a framework for assessing the response of mangroves to relative sea-level rise. *Singap. J. Trop. Geogr.* **42**, 163–183 (2021).

66. Rogers, K. *et al.* Wetland carbon storage controlled by millennial-scale variation in relative sea-level rise. *Nature* **567**, 91–95 (2019).

67. Ouyang, X. & Lee, S. Updated estimates of carbon accumulation rates in coastal marsh sediments. *Biogeosciences* **11**, 5057–5071 (2014).

68. Schuerch, M. *et al.* Future response of global coastal wetlands to sea-level rise. *Nature* **561**, 231–234 (2018).

69. Brown, S. & Nicholls, R. J. Subsidence and human influences in mega deltas: the case of the Ganges–Brahmaputra–Meghna. *Sci. Total Environ.* **527**, 362–374 (2015).

70. Meselhe, E., White, E., Wang, Y. & Reed, D. Uncertainty analysis for landscape models used for coastal planning. *Estuar. Coast. Shelf Sci.* **256**, 107371 (2021).

71. Roe, G. H., Baker, M. B. & Herla, F. Centennial glacier retreat as categorical evidence of regional climate change. *Nat. Geosci.* **10**, 95–99 (2017).

72. Losapio, G. *et al.* The consequences of glacier retreat are uneven between plant species. *Front. Ecol. Evol.* **8**, 616562 (2021).

73. Forbes, D. L. & Syvitski, J. P. *Paraglacial coasts*. (Cambridge University Press, 1994).

74. Strzelecki, M. C. *et al.* New fjords, new coasts, new landscapes: The geomorphology of paraglacial coasts formed after recent glacier retreat in Brepollen (Hornsund, southern Svalbard). *Earth Surf. Process. Landf.* **45**, 1325–1334 (2020).

75. Dümig, A., Häusler, W., Steffens, M. & Kögel-Knabner, I. Clay fractions from a soil chronosequence after glacier retreat reveal the initial evolution of organo–mineral associations. *Geochim. Cosmochim. Acta* **85**, 1–18 (2012).

76. Cauvy-Fraunié, S. & Dangles, O. A global synthesis of biodiversity responses to glacier retreat. *Nat. Ecol. Evol.* **3**, 1675–1685 (2019).

77. Mayer, L. M. Surface area control of organic carbon accumulation in continental shelf sediments. *Geochim. Cosmochim. Acta* **58**, 1271–1284 (1994).

78. Aller, R. C. & Blair, N. E. Carbon remineralization in the Amazon–Guianas tropical mobile mudbelt: A sedimentary incinerator. *Cont. Shelf Res.* **26**, 2241–2259 (2006).

79. Ai, L. *et al.* How did the climate and human activities modulate the sedimentary evolution of the Central Yellow Sea Mud, China. *J. Asian Earth Sci.* 105299 (2022).

80. Luo, X., Yang, S., Wang, R., Zhang, C. & Li, P. New evidence of Yangtze delta recession after closing of the Three Gorges Dam. *Sci. Rep.* **7**, 1–10 (2017).

81. Nittrouer, C. A. *et al.* Amazon sediment transport and accumulation along the continuum of mixed fluvial and marine processes. *Annu. Rev. Mar. Sci.* **13**, 501–536 (2021).

82. Mackenzie, F. T., Ver, L. M. & Lerman, A. Century-scale nitrogen and phosphorus controls of the carbon cycle. *Chem. Geol.* **190**, 13–32 (2002).

83. Lacroix, F., Ilyina, T., Mathis, M., Laruelle, G. G. & Regnier, P. Historical increases in land-derived nutrient inputs may alleviate effects of a changing physical climate on the oceanic carbon cycle. *Glob. Change Biol.* **27**, 5491–5513 (2021).

84. Fennel, K. & Testa, J. M. Biogeochemical controls on coastal hypoxia. *Annu. Rev. Mar. Sci.* **11**, 105–130 (2019).

85. Yao, P. *et al.* Remineralization of sedimentary organic carbon in mud deposits of the Changjiang Estuary and adjacent shelf: Implications for carbon preservation and authigenic mineral formation. *Cont. Shelf Res.* **91**, 1–11 (2014).

86. Hilton, R. G., Galy, A., Hovius, N., Horng, M.-J. & Chen, H. Efficient transport of fossil organic carbon to the ocean by steep mountain rivers: An orogenic carbon sequestration mechanism. *Geology* **39**, 71–74 (2011).

87. Bouchez, J. *et al.* Source, transport and fluxes of Amazon River particulate organic carbon: Insights from river sediment depth-profiles. *Geochim. Cosmochim. Acta* **133**, 280–298 (2014).

88. Keil, R. G. & Mayer, L. M. Mineral Matrices and Organic Matter. in *Treatise on Geochemistry* 337–359 (Elsevier, 2014). doi:10.1016/B978-0-08-095975-7.01024-X.

89. Arndt, S. *et al.* Quantifying the degradation of organic matter in marine sediments: A review and synthesis. *Earth-Sci. Rev.* **123**, 53–86 (2013).

90. Hemingway, J. D. *et al.* Mineral protection regulates long-term global preservation of natural organic carbon. *Nature* **570**, 228–231 (2019).

91. Arnarson, T. & Keil, R. G. Changes in organic matter-mineral interactions for marine sediments with varying oxygen exposure times. *Geochim. Cosmochim. Acta* **71**, 3545–3556 (2007).

92. Bruni, E. T. *et al.* Sedimentary Hydrodynamic Processes Under Low-Oxygen Conditions: Implications for Past, Present, and Future Oceans. *Front. Earth Sci.* **10**, 886395 (2022).

93. Petit, J.-R. *et al.* Climate and atmospheric history of the past 420,000 years from the Vostok ice core, Antarctica. *Nature* **399**, 429–436 (1999).

94. Hilton, R. G. & West, A. J. Mountains, erosion and the carbon cycle. *Nat. Rev. Earth Environ.* **1**, 284–299 (2020).

95. Hemingway, J. D. *et al.* Microbial oxidation of lithospheric organic carbon in rapidly eroding tropical mountain soils. *Science* **360**, 209–212 (2018).

96. Tian, H. *et al.* Increased Terrestrial Carbon Export and CO_2 Evasion From Global Inland Waters Since the Preindustrial Era. *Glob. Biogeochem. Cycles* **37**, e2023GB007776 (2023).

97. Galy, V., Peucker-Ehrenbrink, B. & Eglinton, T. Global carbon export from the terrestrial biosphere controlled by erosion. *Nature* **521**, 204–207 (2015).

98. Bauer, J. E. *et al.* The changing carbon cycle of the coastal ocean. *Nature* **504**, 61–70 (2013).

99. Middelburg, J. J. *Marine carbon biogeochemistry: A primer for earth system scientists*. (Springer Nature, 2019).

100. Wadham, J. L. *et al.* Ice sheets matter for the global carbon cycle. *Nat. Commun.* **10**, 3567 (2019).

101. Hood, E., Battin, T. J., Fellman, J., O'Neel, S. & Spencer, R. G. M. Storage and release of organic carbon from glaciers and ice sheets. *Nat. Geosci.* **8**, 91–96 (2015).

102. LaRowe, D. E. *et al.* Organic carbon and microbial activity in marine sediments on a global scale throughout the Quaternary. *Geochim. Cosmochim. Acta* **286**, 227–247 (2020).

103. Bradley, J. A., Hülse, D., LaRowe, D. E. & Arndt, S. Transfer efficiency of organic carbon in marine sediments. *Nat. Commun.* **13**, 7297 (2022).

104. Laruelle, G. G. *et al.* Global multi-scale segmentation of continental and coastal waters from the watersheds to the continental margins. *Hydrol. Earth Syst. Sci.* **17**, 2029–2051 (2013).

105. Mendonça, R. *et al.* Organic carbon burial in global lakes and reservoirs. *Nat. Commun.* **8**, 1694 (2017).

106. Faust, J. C. *et al.* Millennial scale persistence of organic carbon bound to iron in Arctic marine sediments. *Nat. Commun.* **12**, 1–9 (2021).

107. Suello, R. H. *et al.* Mangrove sediment organic carbon storage and sources in relation to forest age and position along a deltaic salinity gradient. *Biogeosciences* **19**, 1571–1585 (2022).

108. Gu, X. & Brantley, S. L. How Particle Size Influences Oxidation of Ancient Organic Matter during Weathering of Black Shale. *ACS Earth Space Chem.* **6**, 1443–1459 (2022).

109. Kennedy, M., Droser, M., Mayer, L. M., Pevear, D. & Mrofka, D. Late Precambrian oxygenation; inception of the clay mineral factory. *Science* **311**, 1446–1449 (2006).

110. Hage, S. *et al.* High rates of organic carbon burial in submarine deltas maintained on geological timescales. *Nat. Geosci.* **15**, 919–924 (2022).

111. Kleber, M. *et al.* Dynamic interactions at the mineral–organic matter interface. *Nat. Rev. Earth Environ.* **2**, 402–421 (2021).

112. Keiluweit, M. K. G., A., D. & Fendorf, S. Anoxic microsites in upland soils dominantly controlled by clay content. *Soil Biol. Biochem.* **118**, 42–50 (2018).

113. Curry, K. J. *et al.* Direct visualization of clay microfabric signatures driving organic matter preservation in fine-grained sediment. *Geochim. Cosmochim. Acta* **71**, 1709–1720 (2007).

114. Silburn, B. *et al.* Benthic pH gradients across a range of shelf sea sediment types linked to sediment characteristics and seasonal variability. *Biogeochemistry* **135**, 69–88 (2017).

115. Georgiou, K. *et al.* Global stocks and capacity of mineral-associated soil organic carbon. *Nat. Commun.* **13**, 3797 (2022).

116. Hedges, J. I. & Oades, J. M. Comparative organic geochemistries of soils and marine sediments. *Org. Geochem.* **27**, 319–361 (1997).

117. Potter, P. E., Maynard, J. B. & Depetris, P. J. *Mud and mudstones: introduction and overview*. (Springer, 2005).

118. Cai, C. *et al.* Occurrence of organic matter in argillaceous sediments and rocks and its geological significance: A review. *Chem. Geol.* **639**, 121737 (2023).
119. Virto, I., Moni, C., Swanston, C. & Chenu, C. Turnover of intra-and extra-aggregate organic matter at the silt-size scale. *Geoderma* **156**, 1–10 (2010).
120. Bock, M. J. & Mayer, L. M. Mesodensity organo–clay associations in a near-shore sediment. *Mar. Geol.* **163**, 65–75 (2000).
121. Wan, D. *et al.* Effects of long-term fertilization on calcium-associated soil organic carbon: Implications for C sequestration in agricultural soils. *Sci. Total Environ.* **772**, 145037 (2021).
122. Fernández-Ugalde, O. *et al.* Does phyllosilicate mineralogy explain organic matter stabilization in different particle-size fractions in a 19-year C3/C4 chronosequence in a temperate Cambisol? *Geoderma* **264**, 171–178 (2016).
123. Blattmann, T. M. *et al.* Mineralogical control on the fate of continentally derived organic matter in the ocean. *Science* **366**, 742–745 (2019).
124. Yang, J. Q., Zhang, X., Bourg, I. C. & Stone, H. A. 4D imaging reveals mechanisms of clay-carbon protection and release. *Nat. Commun.* **12**, (2021).
125. Blair, N. E., Leithold, E. L. & Aller, R. C. From bedrock to burial: The evolution of particulate organic carbon across coupled watershed-continental margin systems. *Mar. Chem.* **92**, 141–156 (2004).

Corresponding author: Correspondence and requests for materials should be addressed to Thomas Bianchi: tbianchi@ufl.edu

Acknowledgements:

The Jon and Beverly Thompson Chair in Geological Sciences at University of Florida provided support for the TSB.

Table 1:

Table 1. The particulate organic carbon (POC) cycle in the Anthropocene; likely dominated throughout by mud-OC (Box 1). Figure 1 codes are plotted in red on Figure 1. Note that the budget is not closed because it is partly constructed from independent estimates, the contribution of aquatic systems metabolism to burial remains largely unknown, and the timescales of erosion, transport and burial are not uniformized. For instance, mud-OC burial on the continental shelves is timescale dependent as shown quantitatively in [102,103]. "Nearshore" is equivalent to "estuaries and "coastal vegetated ecosystems," while "margins" correspond to "continental shelves". The continental "shelf mask" that we are using covers 28 million km^2 and unambiguously excludes estuaries and anything upstream [104]. Signs for flux with perturbation indicate whether anthropogenic activities have increased (+) or decreased (-) the POC fluxes (?: direction of change unknown).

Figure 1 Code	Landscape Feature/ Process	Flux estimate (TgC yr^{-1})	Flux with perturbation (+/-/?)	From	To	Perturbations	Reference
A	Mountain glaciers	< 1	+	Land	Inland waters	CC	101
B	Land erosion	375	+	Land	Inland waters	CC, LUC	96
C	Dam burial	60	+	Land	Inland waters	CC, LUC, NUT, HYD	28,105
D	Lake burial	90	+	Land	Inland waters	CC, LUC	105

E	Flood plain burial	190	?	Land	Inland waters	CC, LUC, HYD	5,32
F	River export	210	+	Inland waters	Nearshore	CC, LUC, HYD	5,97
G	Permafrost thaw	14	+	Land	Nearshore	CC	55,59
H	Ice sheet erosion	< 5	+	Land	Margins	CC	100
I	Burial in margins	120-180	+	land/nearshore	Margins	HYD, LUC,NUT	5,99
J	Coastal wetland burial	60	-	Land	Nearshore	CUC	5
K	Burial in tidal flats and deltas	50	?	Land	Nearshore	CC, HYD,LUC	5,98

Figure Captions:

Figure 1. Major pathways of mud movement and POC in the Anthropocene; likely dominated throughout by mud-OC (Box 1), and human-induced changes through source-to-sink gradients, modified from [3]. The figure shows the primary locations and movements of mud-OC across landscapes along a conceptual land-to-sea interface. See Table 1 for references and further information associated with these fluxes. Note that the budget is not closed because it is partly constructed from independent estimates, the contribution of aquatic systems metabolism to burial remains largely unknown, and the timescales of erosion, transport and burial are not uniformized. For instance, mud-OC burial on the continental shelves is timescale dependent as shown quantitatively in [102,103]. The red text indicates Table 1 reference: POC flux**,** whether anthropogenic activities have increased

(+) or decreased (-) the POC fluxes (? means direction of change unknown), and source of anthropogenic perturbations: CC = climate and CO_2 increase; LUC: Land-use change; NUT: enhanced nutrients to aquatic systems; HYD: water management; CUC: coastal use change (e.g. reduction in coastal vegetated areas).

Figure 2. Examples of major perturbations of mud-OC pathways. Accommodation space for (a) vegetated coastal ecosystems and (b) deltas is affected by the changing influence of sea-level, sediment accumulation rate, vertical ground motion (c) sediment transport pathways are being altered by anthropogenic alterations, like dam construction, and (d) climate warming and impacts to coastal environments. Plus and negative signals represents increments (+) or reductions (-) on mud-OC fluxes from/to accommodation space associated with different processes that have been altered during the Anthropocene.

Figure 3. Gradients of mud-OC reactivity. a) Typical mud-OC transport timescales for the transit through different environments as derived from radiocarbon measurements (e.g., soil[106], land-ocean aquatic continuum (LOAC)[107–109] , and Shelf[110,111]) calculated based on vertical sinking rates and burial rates (ocean, mixed sediment, sediment). Vertical sinking zones listed on Y-axis are as follows: shelf (0-200 m), slope (200-3000 m), and abyss (>3000 m). b) Distribution of apparent organic matter reactivity as derived from observations, model fitting, and/or laboratory experiments for POC and DOC across different environments over degradation time (e.g., river, catchment, lake, reservoir, wetland[112]), and ocean (sediment traps[113]), sediment[113,114]. The first order degradation rate constant, k, predicted for the respective exposure times by the regional climate model (RCM) model ($k = 0.125\ (0.56\ \text{years} + \text{exposure time})^{-1}$) and the power model ($k = 0.21\ {*}\text{exposure time}^{(-0.985)}$) are indicated by the dashed and solid line, respectively.

Box 1. Definitions of mud and mud-OC

”Mud” is a generic term used differently across scientific and technological disciplines. Here, we consider mud as the finer (<63 μm) components of soils and suspended and deposited sediments. Mud often associates with coarser-grained materials (e.g., sand) to varying degrees and “muds” and “mudstones” are sediments/rocks consisting largely of this finer component. Mud dominates incorporation of other biogeochemically important substances, such as organic carbon, in sediments. We define mud-OC as organic carbon physically associated with mud (e.g., [3]). Mineral-associated organic carbon (MAOC) and particulate organic carbon (POC) are each contained in mud-OC, but also exist in coarser deposits or in suspension. The majority of OC in soil occurs as MAOC, and is generally proportional to mud content [115]. Most sedimentary OC concentrations are similarly related to grain size [116], and mudrocks dominate the sedimentary record [117]; therefore, mud-OC must also dominate global stocks of sedimentary OC. Petrogenic OC from eroded rocks – largely represents fossilized mud-OC associated with clay minerals[3]. Mud-OC occurs in many environments, and can be comprised of terrestrial, marine, and petrogenic sources.

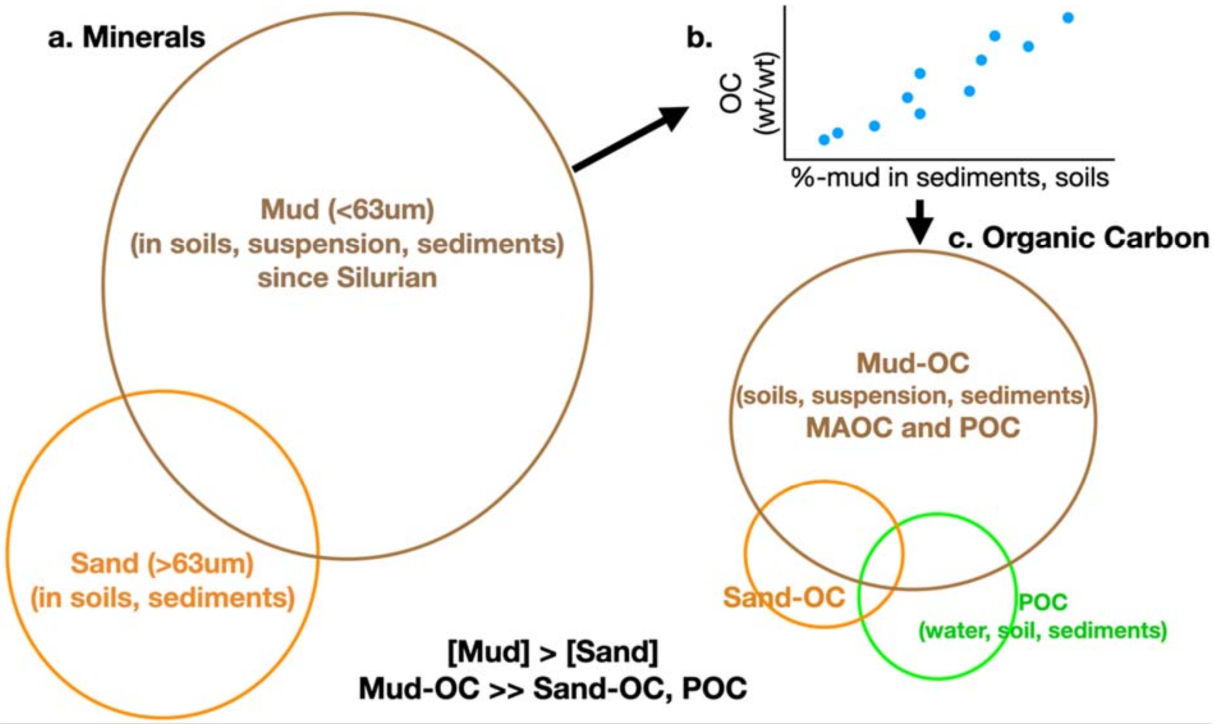

Box 1 figure explanation: The common relationship between OC and mud content of soils and sediment [116,118] (b) combines with the dominance of mud in the sedimentary record [117] (a) to imply the dominance of mud-OC in soils and sediments (c). Mud concentrates and stabilizes OC across rocks, soils, and sediments. Much mud-OC associates with clay and silt-sized minerals or various metals, e.g., iron and calcium, that derive from chemical and physical weathering. Cohesive aggregates develop via physical, chemical and biological mechanisms in soil, riverine, and marine environments[111], with densities between OM and minerals[120]. Aggregation of OM with fine-grained minerals is enhanced by the latter's high specific surface area (SSA) and particle abundance, and affects subsequent transport, settling and compaction. Aggregation can stabilize mud and appears to protect mud-OC against biological degradation[119,120], prolonging OC concentrations and compositions into the rock record[106,109]

The composition, chemical stability, and small size of mud minerals enhance adsorption and occlusion[111,122] . Many bonding types drive adsorption, depending on factors such as local solutes and oxidation state[111], which can change OC reactivity. OC protection also results from its occlusion into compartments that affect access by biota, enzymes and oxidants [111, 112,113] at length scales ranging from adsorption into nm-μm pores to occlusion into mm-scale anoxic microsites to burial in cm-dm-scale, muddy sediment of low permeability. Interactions between adsorption and occlusion make this protection complex[111]. Ratios of OC concentrations to SSA or fine-grained mineral content in bulk soils or sediments allow normalization of OC concentration to mud's protective capability, helping to assess how OC loading in mud changes during source-to-sink transport. Such ratios – e.g., OC:SSA often in the range 0.4-1.0 mg-C/m^2 - respond to factors such as OC supply and oxygen availability[124]. Mud's ability to sequester OC will thus depend strongly on local conditions in the reactors between source and sink.

Box 2. Mud-OC reactivity in the Anthropocene

The reactivity of OC is highly variable and controlled by a plethora of different factors such as OM composition, electron acceptor availability, benthic microbial community composition, physical and physicochemical protection, temperature, microbial inhibition by specific chemicals, priming, and macrobenthic activity. Compiled OC reactivities (e.g., apparent first order OM degradation rate constant k, for OM of concentration G degrading according to a first order rate law of the type: $dG/dt=-k \cdot G$) correlate inversely with exposure to degradation time across highly different environments (Fig. 3), despite inherent variability from a mixture of observations, lab, and modeling data, as well as different approaches in calculating "degradation time". Depositional environments characterized by high, turbulent kinetic energy (enhanced lateral transport), phytodetrital aggregates or mesoscale fronts with enhanced downward transport (enhanced vertical transport) often reveal unusually high apparent benthic OM reactivity (e.g.,[91]). Interestingly, the one to two order of magnitude variances in OC reactivity (y-axis) at various places along the x-axis look consistent across very different environments (e.g., lake sediment vs. wetland) at the century scale. However, human activity such as damming might shunt a certain-age mud from coastal environments that perform as oxidizers to riverine reservoirs of mud-OC. Thus, humans can upshift or downshift the regression line of OC reactivity for any given age material. Changing the residence time of mud therefore puts “a hold” on mud and mud-OC into a different reactivity environment for a new time period. That said, one could shift the apparent “age” of OC by adding younger OC (e.g., autotrophic OC) that would affect the apparent ages from which the plot is constructed. For example, ocean sediment rate constants appear lower than lake sediment ones for <decadal time scales, perhaps due to greater depths of ocean sediments receiving less modern or lower fraction modern (Fm) OC; Fm is the ^{14}C abundance relative to 95% of the activity of NBS Oxalic acid-I in 1950. However, it remains very difficult to predict how this would ultimately affect the x-y regression in Fig. 3 as these effects will vary in intensity and will probably be environment-specific.

A notable example of how humans can rapidly alter the reactivity spectrum of OC across a source-to-sink is the Arctic release of highly reactive, millennial-aged permafrost (e.g.,[10]). If we assume that the fraction of OC that will persist (e.g., will not be accessible on the defined timescale), then changes in transport time scales and environmentally driven changes in degradation rates will have little or no effect. As an example, enhanced downward transport of fresh planktonic OM can have multiple effects on the diagram. One might be via priming (e.g.,[39,36]), and thus accelerating decay of already-present OM. A second might be to induce bottom water anoxia and reduce the reactivity *k* of all of the sedimentary OM.

Methods:

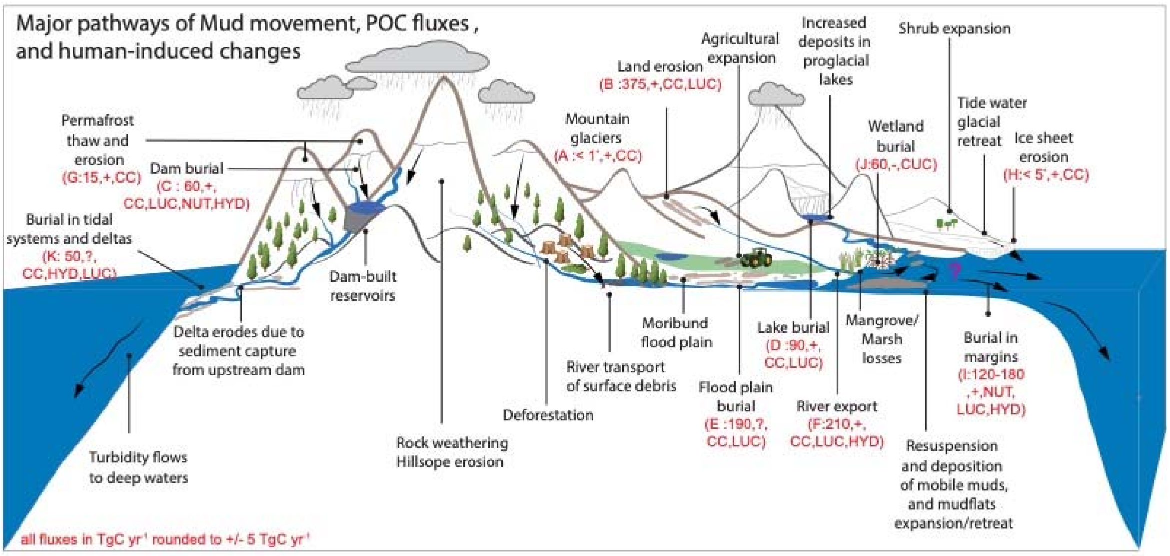

Major pathways of Mud movement, POC fluxes ,
and human-induced changes
Permafrost
thaw and
erosion
(G:15,+,CC)
Dam burial
(C : 60,+,
CC,LUC,NUT,HYD)
Burial in tidal
systems and deltas
(K: 50,?,
CC,HYD,LUC)
Dam-built
reservoirs
Delta erodes due to
sediment capture
from upstream dam
Turbidity flows
to deep waters
Rock weathering
Hillsope erosion
Deforestation
River transport
of surface debris
Moribund
flood plain
Mountain
glaciers
(A :< 1',+,CC)
Land erosion
(B :375,+,CC,LUC)
Agricultural
expansion
Increased
deposits in
proglacial
lakes
Shrub expansion
Tide water
glacial
retreat
Ice sheet
erosion
(H:< 5',+,CC)
Wetland
burial
(J:60,-,CUC)
Flood plain
burial
(E :190,?,
CC,LUC)
Lake burial
(D :90,+,
CC,LUC)
River export
(F:210,+,
CC,LUC,HYD)
Mangrove/
Marsh
losses
Burial in
margins
(I:120-180
,+,NUT,
LUC,HYD)
Resuspension
and deposition
of mobile muds,
and mudflats
expansion/retreat
all fluxes in TgC yr⁻¹ rounded to +/- 5 TgC yr⁻¹

Fig. 1

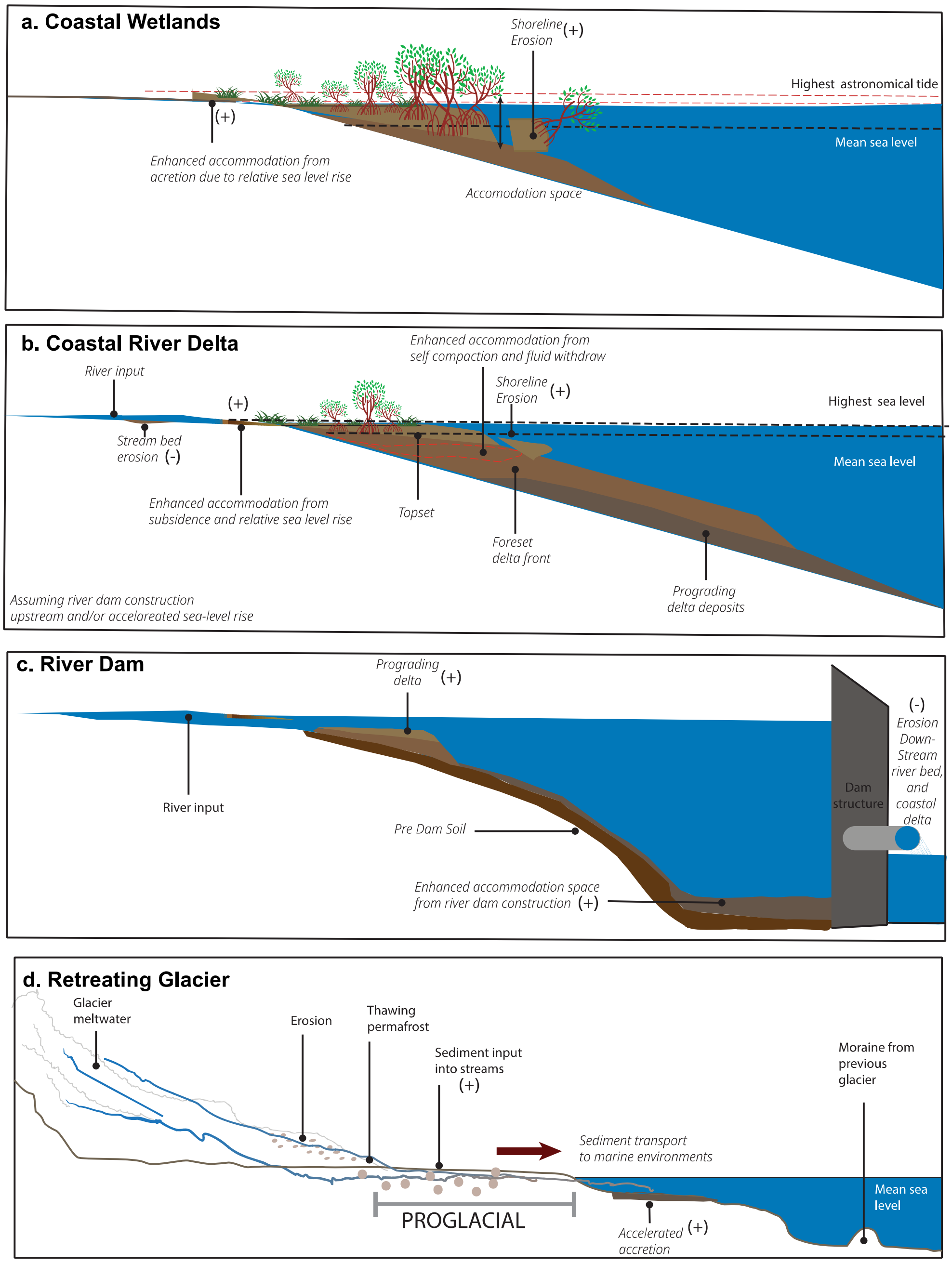
a. Coastal Wetlands
Shoreline Erosion (+)
Highest astronomical tide
Mean sea level
(+)
Enhanced accommodation from acretion due to relative sea level rise
Accomodation space
b. Coastal River Delta
Enhanced accommodation from self compaction and fluid withdraw
River input
Shoreline Erosion (+)
(+)
Highest sea level
Stream bed erosion (-)
Mean sea level
Enhanced accommodation from subsidence and relative sea level rise
Topset
Foreset delta front
Prograding delta deposits
Assuming river dam construction upstream and/or accelareated sea-level rise
c. River Dam
Prograding delta (+)
(-) Erosion Down-Stream river bed, and coastal delta
Dam structure
River input
Pre Dam Soil
Enhanced accommodation space from river dam construction (+)
d. Retreating Glacier
Glacier meltwater
Erosion
Thawing permafrost
Sediment input into streams (+)
Moraine from previous glacier
Sediment transport to marine environments
Mean sea level
PROGLACIAL
Accelerated accretion (+)

Fig. 2

740

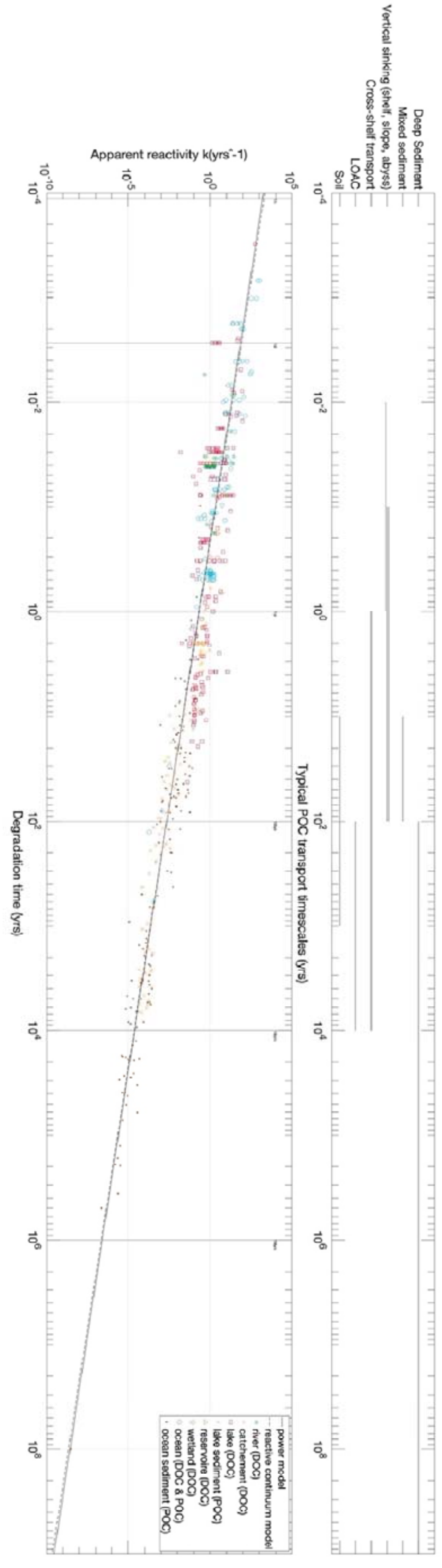

Deep Sediment
Mixed sediment
Vertical sinking (shelf, slope, abyss)
Cross-shelf transport
LOAC
Soil
Typical POC transport timescales (yrs)
Apparent reactivity k(yrs^-1)
Degradation time (yrs)
power model
reactive continuum model
river (DOC)
catchment (DOC)
lake (DOC)
lake sediment (POC)
reservoirs (DOC)
wetland (DOC)
ocean (DOC & POC)
ocean sediment (POC)

Fig. 3